Clim. Past Discuss., 7, 1301–1337, 2011
www.clim-past-discuss.net/7/1301/2011/
doi:10.5194/cpd-7-1301-2011

Climate of the Past Discussions

Using synoptic type analysis to understand New Zealand climate during the Mid-Holocene

D. Ackerley[1], A. Lorrey[2], J. A. Renwick[1], S. J. Phipps[3], S. Wagner[4], S. Dean[1], J. Singarayer[5], P. Valdes[5], A. Abe-Ouchi[6], R. Ohgaito[7], and J. M. Jones[8]

[1]National Institute of Water and Atmospheric Research Ltd, Private Bag 14901, Kilbirnie, Wellington, New Zealand
[2]National Institute of Water and Atmospheric Research Ltd, Private Bag 99940, Newmarket, Auckland 1149, New Zealand
[3]Climate Change Research Centre, University of New South Wales, Australia
[4]GKSS Research Center, Institute for Coastal Research, Paleoclimate Group, Max Planck Strasse 1, 21502 Geesthacht, Germany

[5]Bristol Research Initiative for the Dynamic Global Environment, Geographical Sciences, University of Bristol, Bristol, BS8 1SS, UK
[6]Center for Climate System Research, The University of Tokyo, 5-1-5 Kashiwanoha, Kashiwa, 277-8568, Japan
[7]Japan Agency for Marine-Earth Science and Technology, Showa-machi 3173-25, Kanazawa-ward Yokohama, 236-0001, Japan
[8]Department of Geography, University of Sheffield, UK

Received: 23 March 2011 – Accepted: 11 April 2011 – Published: 19 April 2011

Correspondence to: D. Ackerley (d.ackerley@niwa.co.nz)

Published by Copernicus Publications on behalf of the European Geosciences Union.

CPD
7, 1301–1337, 2011

Abstract

Diagnosing the climate of New Zealand from low-resolution General Circulation Models (GCMs) is notoriously difficult due to the interaction of the complex topography and the Southern Hemisphere (SH) mid-latitude westerly winds. Therefore, methods of downscaling synoptic scale model data for New Zealand are useful to help understand past climate. New Zealand also has a wealth of palaeoclimate-proxy data to which the downscaled model output can be compared, and to provide a qualitative method of assessing the capability of GCMs to represent, in this case, the climate 6000 years ago in the Mid-Holocene.

In this paper, a synoptic weather and climate regime classification system using Empirical Orthogonal Function (EOF) analysis of GCM and reanalysis data, was used. The climate regimes are associated with surface air temperature and precipitation anomalies over New Zealand. From the analysis in this study, we find that increased trough activity in summer and autumn led to increased precipitation, with an increased north-south pressure gradient ("zonal events") in winter and spring leading to drier conditions. Opposing effects of increased (decreased) temperature are also seen in spring (autumn) in the South Island, which are associated with the increased zonal (trough) events. Evidence from the palaeoclimate-proxy data suggests that the Mid-Holocene was characterized by increased westerly wind events in New Zealand, which agrees with the preference for trough and zonal regimes in the models.

1 Introduction

The generation of palaeoclimate-proxy data reconstructions has allowed us to understand how the climate of the past has differed from the present day. By comparing the proxy reconstructions with General Circulation Model (GCM) data, we can evaluate whether the modelled climate is consistent with the palaeoclimate proxy reconstructions. This proxy-model intercomparison is useful because it establishes the veracity of a climate model for representing palaeoeclimatic conditons. This comparison of proxy and model data assists in validating GCMs used to simulate future climate. However, comparing model data with proxy data is difficult, particularly in New Zealand, where the low resolution of GCMs cannot represent the fine-scale topographical features of the land, which are important in governing the regional climate characteristics such as temperature and precipitation (see Mullan, 1998; Salinger, 1980a,b; Salinger and Mullan, 1999). Therefore, a method of bridging the scale gap from coarse resolution GCM to local proxy resolution data, either through downscaling or upscaling, must be employed.

A novel method for "upscaling" regional climate information from proxy reconstructions has been undertaken by Lorrey et al. (2007, 2008). Lorrey et al. (2007) used multi-proxy data to produce regional precipitation anomaly patterns and then related them to the larger scale atmospheric circulation patterns established by Kidson (2000) that are seen on weather time scales. Lorrey et al. (2007) argued there was a self-similar nature to the patterns observed on weather time scales that could be expressed on seasonal and longer timescales. It was hypothesised that the net effect of increased frequency of specific synoptic types would register in proxy archives and reveal the predominant direction of past atmospheric circulation anomalies.

Kidson (2000) used cluster and Empirical Orthogonal Function (EOF) analyses on 12-hourly geopotential height data at 1000 hPa from the NCEP/NCAR reanalysis archive from January 1958 to June 1997 (for more information on the NCEP/NCAR reanalysis see Kalnay et al., 1996) to produce a set of twelve synoptic "weather types" that can be seen in Fig. 1. The work by Kidson (2000) built upon previous studies (see Kidson, 1994a,b; Sturman et al., 1984), which used different sets of synoptic types to those given in Fig. 1. The twelve synoptic types in Fig. 1 come from the study of Kidson (2000) and are the set considered in this study.

The twelve Kidson synoptic types are shown in Fig. 1 as average patterns of 1000 hPa geopotential height (analogous to mean sea-level pressure) from NCEP reanalysis data. Names for the types are indicated in top right of each panel, where

T stands for Trough, SW for Southwesterly, TNW for Trough-North-westerly, TSW for Trough-South-westerly, H for High, HNW for High to the Northwest, W for Westerly, HSE for High to the Southeast, HE for High to the East, NE for North-easterly, HW for High to the West, and R for Ridge. These individual synoptic types can then be grouped into regimes, which are based upon a further cluster analysis (see Kidson, 1997, 2000, for more details)

The three regimes are indicated at the left of Fig. 1: the top row is the trough regime, the first three in the middle row are the zonal regime, and the rest are the blocking regime (see Kidson, 2000, for more details). According to Kidson (2000) trough regimes are associated with above normal precipitation throughout New Zealand and below-normal temperatures. The zonal regime is associated with near-normal-to-cooler temperatures in the North Island and near-normal-to-warmer conditions in the South Island with dry conditions in most places of both islands apart from the far south and west of the South Island. Finally, the blocking regime is associated with generally warmer temperatures throughout New Zealand with reduced precipitation in the southwestern North and South Islands and increased precipitation in the northern and eastern North Island.

The Kidson (2000) synoptic types and regimes were originally defined on a daily basis. However, changes in the synoptic type frequency are associated with distinct regimes that generate regionally disparate precipitation and temperature anomalies in New Zealand climate over months, seasons, and longer periods (demonstrated by Lorrey et al., 2007). The dominance of a particular circulation regime on seasonal, annual or decadal time-scales may therefore be detectable in the instrumental and palaeoclimate-proxy, precipitation and temperature records. Lorrey et al. (2007) demonstrated proof of concept in indicating that such changes in regional climate regime predominance occurred (on low-frequency time scales) as a result of the 1976/1977 Inter-decadal Pacific Oscillation (IPO) phase change. Lorrey et al. (2007) then examined three periods during the last (approximately) 2000 years to infer which basic regional climate regime, and synoptic circulation pattern, may have been

CPD
7, 1301–1337, 2011

dominant on the basis of palaeo-precipitation and temperature records. Such climate regimes and circulation patterns can also be identified from the coarse resolution GCM simulations, which allows a qualitative but direct comparison between the models and multi-proxy data assemblages that underpin regional climate regime classification (Lorrey et al., 2007, 2008).

Many global modelling groups have produced valuable GCM simulations for representations of the Mid-Holocene (6000 years before present, ybp) and the Last Glacial Maximum (21 000 ybp), which are stored as part of the Palaeoclimate Modelling Intercomparison Project (PMIP, see Joussaume and Taylor, 2000). Despite the large archive of model data (see Braconnot et al., 2007, for an overview of the PMIP2 model results), there have been relatively few studies of the Southern Hemisphere (SH) climate (for examples see Ackerley and Renwick, 2010; Rojas et al., 2009) from the PMIP2 data. There have however been some studies of the SH westerlies from other model simulations (Wagner et al., 2007; Wardle, 2003). Given the issues in representing SH mid-latitude circulation in GCMs (see Randall et al., 2007), and the sparsity of SH observational data, methods of assessing GCM simulations in comparison to instrumental or proxy records are very important. The use of different climate models is essential for investigations on natural climate variability because of the differences in mean climate and the model-inherent biases. To reduce the uncertainty concerning model specific features, we use four different models that have also been used (partly) in PMIP. In addition to PMIP, we use the model output to statistically downscale the large-scale atmospheric circulation to the local climate in New Zealand. This should help to discriminate between real climatically induced climate changes (due to changes in external forcing) and model-specific features, which are potentially unrelated to the combination of naturally forced internal and external climate variability.

The aim of this study therefore, is to provide a first step for assessing SH circulation patterns as represented by a set of GCMs that cover the Mid-Holocene. These patterns are then compared to palaeoclimate proxy data within the New Zealand sector. Ackerley and Renwick (2010) have already shown that the seasonal SH

CPD
7, 1301–1337, 2011

mid-latitude circulation is sensitive to differences in the Earth's orbital paramaters during the Mid-Holocene, which is caused by changes in seasonal insolation (see Fig. 2). We would therefore expect the frequency of synoptic types shown in Fig. 1 to change during the Mid-Holocene. To test this hypothesis we will assess if the synoptic type frequency in the New Zealand sector has changed and relate these changes to seasonal climate regimes, from which regional precipitation and temperature patterns can be inferred. A further test of the synoptic type frequency changes during the Mid-Holocene, as determined by the model ensemble, is to then compare the results to past conditions established by palaeoclimate regime reconstructions for the same time period.

A description of the models used in this analysis and the data provided can be found in Sect. 2. An analysis of the seasonal differences in the climate regimes can be found in Sect. 3 along with their relation to the wider SH circulation. A discussion of the implications for New Zealand temperature and precipitation from the results in Sect. 3, will be given in Sect. 4 and the main conclusions will be given in Sect. 5.

2 Models, data and method

2.1 CSIRO Mk3L

The CSIRO Mk3L climate system model is a fully-coupled atmosphere-sea ice-ocean general circulation model. It comprises atmospheric and oceanic general circulation models, a dynamic-thermodynamic sea ice model and a land surface scheme with static vegetation. The atmosphere model has a horizontal resolution of $5.6^{\circ} \times 3.2^{\circ}$ and 18 vertical levels, while the ocean model has a horizontal resolution of $2.8^{\circ} \times 1.6^{\circ}$ and 21 vertical levels. Further details of the CSIRO Mk3L model used here can be found in Phipps (2010).

The pre-industrial control simulation used orbital parameters for 1950, while the Mid-Holocene experiment used orbital parameters for 6000 years before present (ybp). For both experiments, the solar constant was set to 1365 Wm^{-2} and the CO_2 concentration was set to 280 ppm. The model does not explicitly represent the radiative effects of CH_4 or N_2O.

Fifty years of sea level pressure (SLP) data sampled at 00:00 UTC each model day along with monthly mean surface air temperature at 2 m were provided for this analysis.

2.2 ECHO-G

ECHO-G is a fully coupled ocean-atmosphere GCM (Legutke and Voss, 1999), which has been used in Wagner et al. (2007) to carry out transient simulations of the Mid-Holocene. The atmospheric component is a version of ECHAM4 (Roeckner et al., 1996), which is triangularly truncated with a wavenumber of 30 (T30 approximately 3.75° longitude by 3.75° latitude) and has 19 vertical levels. The ocean component is a version of HOPE-G (Wolff et al., 1997) with 2.8° horizontal resolution (both in longitude and latitude) and 20 vertical levels. In order to better represent effects related to ENSO a grid refinement is employed in the tropics and resolution increases here to 0.5°. To prevent climate drift the model is also flux adjusted, as described in Wagner et al. (2007).

The data in this study are taken from a simulation only driven with changes in orbital variations. The model was integrated from 7 ka BP to 4.5 ka BP with a solar constant set to 1365 Wm^{-2} and greenhouse gas concentrations of 280 ppm for CO_2, 700 ppb for CH_4 and 265 ppb for N_2O. The data from 6000 ybp – 5950 ybp were compared to a pre-industrial simulation forced with the same solar constant and greenhouse gas concentrations as used in the Mid-Holocene simulations but with orbital parameters reflecting conditions of 1750 AD. Daily mean sea level pressure and 2 m surface air temperature were taken from 6000 ybp to 5950 ybp.

CPD

7, 1301–1337, 2011

2.3 HadCM3_UB

HadCM3_UB is a fully coupled ocean-atmosphere GCM. The atmospheric component is a hydrostatic grid-point model with a resolution of 3.75°longitude, 2.5°latitude and 19 vertical levels. The ocean model has a horizontal resolution of 1.25°(both longitude and latitude) and 20 veritcal levels. Further details of the Hadley Centre model and the parameterized processes can be found in Gordon et al. (2000).

Daily mean SLP data were provided from the simulation used in the PMIP2 experiment for the Mid-Holocene run and a pre-industrial (circa 1750) control run. The solar constant was set to 1365 Wm^{-2} and, CO_2 and N_2O concentrations were set to 280 ppm and 270 ppb (respectively), in both data sets. The orbital parameters were perturbed between the two simulations (Mid-Holocene and pre-industrial, see Table 1 in Braconnot et al., 2007) as were the CH_4 concentrations (760 ppb for the pre-industrial and 650 ppb for the Mid-Holocene). Further details of the model setup can also be found in Singarayer and Valdes (2010). 100 years of daily mean SLP data were provided from both simulations along with monthly mean surface air temperature data.

2.4 MIROC

The MIROC model is also a fully coupled ocean-atmosphere GCM, which has a triangularly truncated atmosphere with a wavenumber of 42 (T42 approximately 2.8°longitude by 2.8°latitude) and 20 vertical levels. The ocean model has a horizontal resolution of 1.4°longitude, 0.5°latitude and 43 vertical levels. Details of MIROC can be found in the technical report by the K-1 Developers (K-1 model developers, 2004).

Both the Mid-Holocene and pre-industrial experiments were set up with the same conditions as those given for HadCM3_UB (also see Ohgaito and Abe-Ouchi, 2007, for more details) in Sect. 2.3 (following the guidelines from PMIP2). Again, 100 years of SLP data were provided along with monthly mean surface air temperature data.

CPD
7, 1301–1337, 2011

2.5 EOF proceedure for synotic classification

The EOF analysis used by Kidson (2000) requires 1000 hPa geopotential height data, and while SLP is analogous to 1000 hPa geopotential height it is not the same. The model-output SLP data were converted to equivalent 1000 hPa height, using the monthly mean surface air temperature provided. The classification proceedure documented in Kidson (1997, 2000) is then run on the converted SLP data, which assigns the "closest" synoptic type from Fig. 1 to each day of the data sets. The "closest" synoptic type is calculated as the minimum Euclidian distance to the mean height field associated with each of the synoptic types. The distance is calculated in terms of the first five principal components of the 1000 hPa height field (see Kidson, 1997, 2000, for more details).

The output from the synoptic classification proceedure is considered on a seasonal basis where the austral seasons are defined to be December-January-February (DJF, summer), March-April-May (MAM, autumn), June-July-August (JJA, winter) and September-October-November (SON, spring). The totals in each season for each year can then be summed to give the total frequency of occurrence of synoptic types in each regime, during the Mid-Holocene and pre-industrial simulations (see Table 1). Changes in regional New Zealand climate therefore can be inferred from systematic changes in the frequency of occurrence of the individual synoptic types on weather time scales (based on the relationships between the Kidson, 2000, types and modern observations). Application of the same anomalies to the Mid-Holocene follows uniformitarianism principles that suggest similar changes would result in climate regime shifts over longer time periods. Ackerley and Renwick (2010) found that the strongest changes in the SH circulation occurred in SON and MAM, and were associated with the sea-surface temperature response to the changes in insolation shown in Fig. 2. Therefore, we expect the largest changes in the synoptic regimes to occur in SON and MAM but all seasons will be considered.

CPD
7, 1301–1337, 2011

3 Results

The seasonal frequency of occurrence and the difference between the Mid-Holocene (MH) and pre-industrial (PI) control runs, for each of the synoptic regimes given in Sect. 1, can be seen in Table 1. The differences in the frequency of occurrence were subjected to a z-test for two proportions. Changes that are statistically significant ($p \leq 0.05$) have an asterisk. For comparison with the results in Table 1, the difference in sea level pressure (SLP) for the MH relative to the PI, for each of the seasons, can be seen in Figs. 3–6. These changes in SLP were subjected to a t-test for equal means and statistically significant changes in SLP ($p \leq 0.05$) for the MH relative to the PI are shaded grey.

The seasonal frequencies of occurrence for the NCEP reanalysis data (over the period 1972–2009) are given in Table 1. The models do reasonably well at capturing the seasonal variation in the regime frequencies as an ensemble mean. However, there are obvious differences between the individual models and the NCEP data and generally the models do better in MAM and SON than in DJF and JJA. The cause of some of the differences may be due to the models representing a pre-industrial climate (circa 1750), whereas NCEP data are for present day. Therefore, the discussion will focus on the coherent changes in the regimes that are common to all of the models (or most of them). While we accept that the models are subjected to specific errors and biases, if the ensemble of models show a coherent pattern of distinct regime change it will increase our confidence in their representataion of past climate. Each season will be analysed separately with respect to Table 1 and the pressure patterns in Figs. 3–6. The largest changes in the individual synoptic types (see Fig. 1) will also be discussed where appropriate, although exact values for these will not be quoted as they are used qualitatively to understand the SLP anomalies.

CPD
7, 1301–1337, 2011

3.1 DJF

In DJF, all models except ECHO-G have an increase (statistically significant) in the number of trough synoptic types. Also, all models except MIROC have a statistically significant decrease in the zonal regime synoptic types.

The pressure anomaly maps for CSIRO Mk3L and MIROC (Fig. 3a and d) have a much more zonally symmetric increase in SLP throughout the SH high-latitudes with decreases to the north. The pattern is stronger in CSIRO Mk3L than MIROC, which explains why CSIRO Mk3L has a stronger increase in trough synoptic types than MIROC. However, while CSIRO Mk3L has an equivalent decrease in the zonal regime to the increase in the trough regime MIROC does not, and loses blocking events to trough events.

For ECHO-G, high-latitude SLP is reduced in DJF for the MH compared to the PI, and the reduction in trough synoptic types agrees with the pressure pattern in Fig. 3b. However, the large (and statistically significant) high anomaly centred to the south and west of New Zealand (and extending to the east) agrees with the decrease in the zonal regime too, and consequently an increase in blocking (the majority of which come from HSE events).

Finally, HadCM3_UB has increases in trough synoptic types, in agreement with reduced SLP in the New Zealand region (Fig. 3c), and decreases in zonal synoptic types (similar to CSIRO Mk3L). However, the changes in SLP are much less zonally symmetric in HadCM3_UB than CSIRO Mk3L (compare Fig. 3a and c) and the overall changes in SLP are weaker, which agrees with the smaller magnitude values of DT and DZ in Table 1 for HadCM3_UB.

3.2 MAM

The MAM changes in the synoptic regimes are stronger and more coherent across all of the models, than in any other season (and the season for which the models are in best agreement with NCEP). All the models have a statistically significant increase in

CPD
7, 1301–1337, 2011

troughs and a decrease in zonal synoptic types, with three out of the four models also having a statistically significant decrease in blocking occurrence (see Table 1).

The changes in the synoptic regimes also agree very well with the changes in the pressure patterns in all of the models (Fig. 4a–d). All models have an increase in SLP throughout the SH high-latitudes in the MH compared to PI, with strong decreases in SLP centred to the east of New Zealand, which extend throughout much of the SH mid-latitudes. While all of the models have increased trough frequency, the models with the more zonally symmetrical changes in SLP (CSIRO Mk3L, ECHO-G and MIROC – Fig. 4a, b and d) have the largest increases in T events, whereas HadCM3_UB (which is much less zonally symmetric, Fig. 4c) has the largest increase in TSW events.

All the models have a large reduction in the occurrence of H (zonal) and HSE (blocking) events, which agrees with the general pattern of reduced pressure in the New Zealand region. However, the loss of H events in HadCM3_UB is countered by an equal increase in R-type patterns, which suggests that the wave number three pattern in Fig. 4c is not a stationary feature, and high anomalies can propagate from west to east across New Zealand.

3.3 JJA

In JJA all models have a decrease in the frequency of troughs, of which three have a statistically significant decrease (see Table 1). Also, three of the four models have a statistically significant increase in the zonal regime.

The changes in SLP for the MH relative to the PI are more complex for each of the models than in any of the previous seasons (see Fig. 5a–d). The three models that have a statistically significant reduction in troughs all have increases in SLP for the MH compared to the PI (ECHO-G, HadCM3_UB and MIROC in Fig. 5b–d), close to New Zealand. The CSIRO Mk3L model, however, has a decrease in the number of blocking synoptic types and an increase in zonal synoptic types. The largest contributor to this change is a decrease in the number of HSE and NE events, and an increase in H events, which agrees with increased (decreased) SLP to the west (east) of New Zealand in Fig. 5a.

The ECHO-G and HadCM3_UB models also have more H events (particularly in HadCM3_UB) but ECHO-G also has a similar increase in HNW events too, which agrees with the high SLP anomaly in Fig. 5b being displaced more to the west than in Fig. 5c. Finally, the MIROC model has less HNW and W events, which agrees with the southern displacement of the high SLP anomaly in Fig. 5d, with the increase in blocking caused mainly by an increase in HSE events.

3.4 SON

For SON, all of the models have a decrease in the frequency of troughs and an increase in the frequency of zonal synoptic types, which are all statistically significant (and large in magnitude). While ECHO-G and MIROC do not have statistically significant changes in the blocking regime, both CSIRO Mk3L (increase) and HadCM3_UB (decrease) do. The causes of these differences can be understood by looking at the changes in SLP for the MH compared to the PI, and also by identifying which of the individual synoptic types in Fig. 1 have changed the most. The changes in SLP for SON are given in Fig. 6 and (in all cases) there are increases around New Zealand, which agrees with the reduction in troughs. While ECHO-G and HadCM3_UB have a reduction in high-latitude SLP (see Fig. 6b and c), CSIRO Mk3L and ECHO-G (Fig. 6a and d) indicate an increase.

In all models, the frequencies of H, HNW and W synoptic types increase from PI to MH (particularly in H and HNW) and all synoptic types in the trough regime decrease for all models except HadCM3_UB. In HadCM3_UB there is a strong increase in the frequency of the SW type and a decrease for all synoptic types in the blocking regime, which agrees with the pressure anomaly pattern in Fig. 6c. In CSIRO Mk3L, there are strong increases in the HSE and HE types for blocking, which agrees with the high pressure anomaly situated to the east of New Zealand in Fig. 6a. In MIROC however, (which has a similar SLP anomaly pattern to CSIRO Mk3L, Fig. 6d) the increases

CPD
7, 1301–1337, 2011

in HSE and HE events are offset by reductions in NE and R. Finally, while ECHO-G has a reduction in high-latitude SLP in SON (Fig. 6b), the SLP anomalies are more zonally symmetric, which causes a decrease (increase) in trough (zonal) types with little change to the occurrence of blocking types.

3.5 Summary

Generally, the climatic pattern from the results given above implies more disturbed conditions for New Zealand during the Mid-Holocene. The models indicate an increase in zonal types in JJASON, which implies strengthened westerlies, and more trough events in DJFMAM suggesting unsettled conditions. The lack of a coherent seasonal signal in the blocking regime (except in MAM where three of the four models have a decrease in blocking events) also agrees with the more disturbed pattern near New Zealand during the Mid-Holocene.

4 Implications for New Zealand

4.1 Downscaled changes in temperature and precipitation

Having identified how the synoptic regimes differed seasonally in the MH compared to the PI in the GCMs, we can infer how the seasonal climate may have been different in New Zealand during the Mid-Holocene. Originally, Kidson (2000) estimated the anomalies in temperature and precipitation associated with each synoptic regime, regionally for New Zealand from monthly mean data. Trough events were associated with generally wetter conditions throughout New Zealand and cooler conditions in the south. Zonal events are associated with drier conditions in the north and east of New Zealand with warmer conditions in the south. Finally blocking events were associated with generally warmer temperatures throughout New Zealand with reduced precipitation except in eastern parts of both the North and South Islands and the north of the North Island.

CPD
7, 1301–1337, 2011

The analysis undertaken by Kidson (2000) was repeated in this study using daily SLP data from the NCEP/NCAR reanalysis and daily temperature and precipitation data from the Virtual Climate Station Network (VCSN, see Tait et al., 2006, for a description of the methodology) in New Zealand from 1972 to 2009. The daily VCSN fields were averaged by regime type and season to produce a downscaled mean field of temperature and rainfall patterns for the present day. We then applied the percentage change in the frequencies of occurrence of each regime, for each model in Table 1 (DT, DZ and DB), to produce the likely temperature and precipitation anomalies for the Mid-Holocene relative to the present day. The anomalies were then averaged across the models to produce an ensemble mean anomaly, which can be seen in Figs. 7 and 8 for temperature and precipitation in each season.

The higher incidence of trough events in MAM during the Mid-Holocene causes an increase in surface air temperature throughout the North Island (particularly in the east) and a decrease throughout much of the South Island (particularly in the south and west) and can be seen in Fig. 7. Conversely, the higher incidence of zonal synoptic types in SON during the Mid-Holocene induces a slight cooling in parts of the North Island and strong warming of the South Island (again, particularly in the south and west). In both cases (MAM and SON), the warming and cooling are ~0.2°C in magnitude and even weaker in DJF and JJA.

The values in Fig. 7 only account for the temperature changes caused by differences in circulation, whereas the model data includes changes in temperature from a combination of circulation and insolation differences. While the low resoution of the models does not allow us to understand the fine structure of the temperature changes; large scale cooling or warming, primarily driven by changes in insolation, may enhance or reduce the temperature variations seen in Fig. 7. The suggestion from the models is that surface air temperatures in the New Zealand region were at least 0.2°C cooler in DJF through to JJA (not shown) due to circulation changes and reduced insolation (see Fig. 2 for insolation changes), which suggests that the reduced insolation may have the dominant effect on temperature in DJF to JJA. In SON, the models suggest

CPD
7, 1301–1337, 2011

a small warming around New Zealand of ∼0.1°C due to changes in circulation and increased insolation, which suggests that the insolation increases in SON (see Fig. 2) may slightly enhance the South Island warming seen in Fig. 7 .

Despite the overall South Island warming in SON, the influence of HNW synoptic types relative to W types (noted in Sect. 3.4) suggests an increase in southwesterly flow over New Zealand during SON relative to westerly and northwesterly flow. While the tendency is for a warmer South Island during SON (see Fig. 7) in the Mid-Holocene, HNW types are associated with increased frost occurrence (not shown) throught the southern and western South Island in particular. Therefore, New Zealand may have been prone to more frequent frost outbreaks during spring in the Mid-Holocene relative to the present, despite the overall tendency for warmer conditions in the South Island. The weakest overall anomalies occur during DJF, where there are only very small changes in temperature resulting from the increases in trough synoptic types.

Overall, it seems likely that the seasonal insolation changes (see Fig. 2) may have had a larger influence on surface air temperature than the changes in the synoptic regimes. However, the high spatial variability of the changes in temperature given in Fig. 7 indicate that the synoptic regimes may have enhanced or reduced the magnitude of the temperature responses to the changes in insolation. The coarse resolution of the GCMs does not allow us to investigate these local changes.

Whereas the differences in temperatures were quite weak, the precipitation anomalies associated with the Mid-Holocene climate regimes are more prominent (Fig. 8). The increase in trough occurrence for MAM during the Mid-Holocene suggests that increased precipitation was more likely throughout New Zealand compared to present day. Similarly, there are positive precipitation anomalies throughout New Zealand in DJF too, which indicates a wetter DJFMAM than at present associated with the increase in the trough regime. However, the increase in the frequency of zonal events causes a strong drying for many parts of the North and South Islands in SON, although the drying is reduced (or even reversed) in the far south and west of the South Island. A similar pattern can also be seen in JJA (albeit weaker) in agreement with the smaller

CPD
7, 1301–1337, 2011

changes in Table 1. Overall, the model output suggests wetter conditions throughout New Zealand in DJFMAM and drier conditions during JJASON, which agrees with the suggested reduction in SH seasonality identified in Braconnot et al. (2007) for the Mid-Holocene.

4.2 Implications from the New Zealand palaeoclimate record

A suite of proxy reconstructions of environmental change from across New Zealand were recently summarised by Li et al. (2008), who suggested national-scale precipitation and temperature regime changes occurred in the Mid-Holocene. They demonstrated a key environmental shift occurred in the Mid-Holocene, and suggested this change was a causal mechanism for vegetation change at Sponge Swamp in the western South Island (WSI) regional climate district. At that site, a significant drop in the pollen representation of the small tree *Ascarina lucida* began at ~6.9 ka, and there was also a change in peat deposition beginning at ~6.4 ka. The interpretation of the *Ascarina change* follows multiple studies (McGlone et al., 1988; Newnham et al., 1989; Martin and Ogden, 2002, 2005) that demonstrate this species needs warm and wet conditions (with limited frost exposure) to survive, and regeneration is dependent on disturbance events. Similarly, the decline or disappearance of *Ascarina* can also be used to imply a shift to cooler or drier times, increased frost incidence or low disturbance. The interpretation provided by Li et al. (2008), suggesting reduced humid northerly flow and increased southwesterlies, is similar to that of McGlone et al. (1993), who suggested at some time between ~7.5 to 3 ka, key environmental shifts occurred in many northern and western areas and that there were wetter winters, a slight cooling in climate, and an increase in southerly fronts and frosts in New Zealand.

Pollen profiles from interior Canterbury adjacent to the eastern edge of the WSI climate district (Burrows and Russell, 1990) and in the Takitimu Mountains in Southland (Vandergoes et al., 1997) show elevated pollen from *Prumnopitys taxifolia* (matai; a tall conifer) in the early Holocene. *P. taxifolia* environmental affinities in New Zealand tree distribution models indicate it reaches maximum abundance in drought-prone climates

CPD
7, 1301–1337, 2011

at sites with large air saturation deficits (Leathwick and Whitehead, 2001). The pollen abundance of this species has also been interpreted as past dry periods (Horrocks and Ogden, 1998), suggesting the WSI experienced significant dry anomalies prior to 6 ka. *P. taxifolia* declined in synch with a rise of *Nothofagus menziesii* at many sites in the WSI after ∼6 ka (Harris, 1963; McGlone and Bathgate, 1983; Burrows and Russell, 1990; Vandergoes et al., 1997).

Lorrey et al. (2008) recently provided an overview of the way *N. menziesii* and *P. taxifolia* could be employed as contrasting climate change indicators. *N. menziesii* (silver beech) is a frost tolerant species that can survive sub-zero temperatures (Neuner et al., 1997; Sun and Sweet, 1996). It is also a drought-intolerant species, which may lead to its exclusion from lowland sites in warm, dry areas throughout New Zealand (Manson, 1974), and mass mortality of this type of tree has also been attributed to severe drought episodes (Jane and Green, 1983, 1984). The combination of frost tolerance and drought intolerance results in *N. menziesii* being the most abundant *Nothofagus* species at high altitude sites with poor soil drainage (Ogden et al., 1996). While temperature may play a role in determining the distribution of *N. menziesii*, the defining environmental differences of *N. menziesii* and *P. taxifolia*, and one reason for their apparent contrast in pollen diagrams covering the Mid-Holocene, appears to relate to their drought tolerances. Both species can be abundant at cold sites or during periods of reduced temperatures, but *N. menziesii* is abundant at sites where soil water deficits are rare, and *P. taxifolia* thrives in drought-prone regions or in drier climatic intervals. The beech expansion and *P. taxifolia* decrease seen in the Mid-Holocene at approximately 6 ka, along with the other evidence summarised by Li et al. (2008) and McGlone et al. (1993) indicate a circulation occurred that supported a change from drier to wetter conditions in the WSI. Decreased tall tree pollen and increased *Coprosma* (and other small trees/shrubs) along with observations of woody debris layers in peat cores from the southern South Island also suggest increased disturbance due to more frequent westerly wind storms and more precipitation in WSI during the Mid-Holocene (McGlone and Bathgate, 1983). In addition, Schaefer et al. (2009) have presented cosmogenic

CPD
7, 1301–1337, 2011

surface exposure age dates for the Tasman and Mueller glaciers that indicate an ice advance occurred at approximately 6520 ± 360 years ago, which also suggests a climate regime change that favoured lower temperatures and increased precipitation in WSI (weighted to summer) would have occurred in the Mid-Holocene close to ∼6 ka.

Overall, the palaeo-vegetation and glacial evidence suggests a circulation regime shift (albeit non-synchronous at many sites due to differing chronologic controls and sample resolution employed for the palaeoclimate archives) that favoured more frequent westerly and southwesterly circulation, which are hallmarks of zonal and trough synoptic types. Increased zonal and trough events would have brought an increase in precipitation in western and southern regions, an increase in the occurrence of southerly fronts, cooler temperatures and increased incidents of frost for WSI at ∼6 ka. This palaeoclimate evidence is consistent with increased zonal and trough activity observed in the palaeoclimate model simulations presented in this study. The palaeoclimate evidence summarised here and the results from the model synoptic type frequency comparison reconcile a critical proxy-model discrepancy previously noted by McGlone et al. (1993). In that study, CLIMAP SST results suggested increased seasonality and decreasing westerly windflow at ∼6000 years before present in the New Zealand sector, while land-based palaeovegetation records implied increased seasonality, increased windiness, and increased southerly quarter windflow. Our results are based on model outputs that are obviously more advanced, have finer spatial resolution, and have more detailed information about atmospheric circulation patterns relative to the CLIMAP results that have improved proxy-model comparisons for New Zealand. The palaeoclimate model ensemble collectively indicates that an increase in westerly and southerly quarter flow due to more frequent trough and zonal circulation, was likely at ∼6 ka, and the proposed circulation change agrees with precipitation- and temperature-sensitive climate proxies for the same time period. On a larger spatial scale, the timing of a Mid-Holocene transition, observed in New Zealand, to increased westerly and southerly quarter influences was also seen in Chile (Lamy et al., 2001). We hypothesise that the similar timing of changes observed at distal locations across

CPD
7, 1301–1337, 2011

the Pacific Basin (that include the regionally-distinct, synoptic circulation-driven shifts in New Zealand at ∼6 ka) were nested within a large-scale hemispheric-scale circulation mode. Future efforts to expand the regional climate regime classification approach (Lorrey et al., 2007, 2008) across the Southern Hemisphere, and a subsequent comparison of the proxy-based patterns with large scale palaeoclimate model results, could help to reveal the timing and refine the character of distinct hemispheric-circulation modes that occurred in the past.

5 Conclusions

This study has shown that the seasonal circulation characteristics over New Zealand were different during the Mid-Holocene compared to the pre-industrial era with coherent patterns between four GCMs. However, while the changes in the synoptic regimes are consistent between the models, there are large differences in which of the individual weather types is contributing the most to those changes (as discussed in Sects. 3.1–3.4). The differences in the individual types agree with the SLP anomaly patterns discussed in Sect. 3 but the summation of the frequencies of occurrence across the regimes does not account for the individual changes. Overall, the strongest changes in the circulation occurred in MAM and SON, with weaker differences in DJF and JJA.

There were statistically significant increases in troughs for all models during MAM and for three of the four models during DJF. The changes in the regimes resulted in increased precipitation during DJFMAM and much colder South Island temperatures in MAM. There were also statistically significant increases in zonal types for all models during SON and for three out of four models in JJA. The increase in zonal flow is likely to have caused drying throughout much of New Zealand in JJASON (except in the western South Island) and warming of the South Island in SON. However, the combination of increased trough events in DJFMAM and zonal events in JJASON may have caused increased rainfall throughout the year in the extreme south and west of the South Island and an overall depression in mean annual temperature.

Overall, the precipitation and temperature anomalies in DJFMAM and JJASON may cancel out over most of New Zealand when considering the annual mean. This is similar to the results seen for the modern reanalysis period that indicated the most significant climate regime shifts were on sub-annual time scales, and that there was no statistically significant change in synoptic type frequency when comparing annual statistics for opposite IPO phases (Lorrey et al., 2007). However, the suggestions from the proxy reconstructions discussed in Sect. 4.2 are that:

– There was a shift to cooler conditions at some point during the Mid-Holocne close to ~6 ka.
– Conditions were likely to have been more "disturbed" with increased westerly wind storms.
– Lower temperatures, increased incidence of frost and increased precipitation in the western South Island resulted from circulation change.

Despite an overall lack of change in the frequency of occurrence of each of the weather regimes (as the seasonal differences cancel somewhat), the inferred climate from the proxy reconstructions is consistent with the model output. While there is no evidence of an overall shift to cooler temperatures in the models, there is evidence for a cooler autumn in the South Island. Another contributing factor may have been the difference in the Earth's orbital parameters during the Mid-Holocene, which caused lower insolation for the SH during DJFMAM and may have led to further cooling. Also, despite the suggested warming in the South Island from the changes in the modelled regimes, the increase in HNW synoptic types may have increased frost occurrence in spring (particularly in the western South Island), which also agrees with the proxy data. However, due to the low resolution of the GCMs used in this study, they are not able to represent the detailed topographical features of New Zealand and so we cannot confirm the changes in precipitation and temperature directly from the models. Further improvement could be attained with the use of dynamical downscaling (for example

CPD
7, 1301–1337, 2011

with a regional climate model), which would also include the different solar forcing of the Mid-Holocene compared to the present day. However dynamical downscaling is currently beyond the scope of this paper.

There is also evidence in the models for year-round disturbance (in agreement with the proxy data) with increases in trough regime influence in DJFMAM and zonal regime predominance in JJASON with little consensus between the models for changes in blocking frequency. Therefore, despite there being little change annually to the synoptic regimes (and subsequently temperature and precipitation inferrred from this study), there is evidence for more unsettled conditions in DJFMAM and intensified westerly winds in JJASON.

Despite the low resolution, the classification of synoptic weather types into climate regimes and associated qualitative downscaling to regional climate variability (including the regionally contrasting patterns that arise from orographic effects) is a first step in understanding the possible changes in New Zealand climate during the Mid-Holocene and identifying underlying causes of the changes. The method used in this study will also allow us to compare the model output with proxy time slices that are generated in a similar manner to Lorrey et al. (2007). Also, the use of GCM simulations to undertake dynamical downscaling (for example using a regional climate model) may add further insight into the climate of New Zealand during the Mid-Holocene.

Acknowledgements. This work contributes to the Adaptation to Climate Variability and Change programme (contracts C01X0202 and C01X0701), Modelling Palaeoclimate to Inform the Future programme (contract UOAX0213), and the Regional Climate Modelling to Develop Probabilistic Scenarios of Future New Zealand Climate (contract C01X0804) programme. The authors would also like to thank Georgina Griffiths for providing useful input in reviewing a draft version of this paper.

CPD
7, 1301–1337, 2011
New Zealand climate in the Mid-Holocene
D. Ackerley et al.

References

Ackerley, D. and Renwick, J. A.: The Southern Hemisphere semiannual oscillation and circulation variability during the Mid-Holocene, Clim. Past, 6, 415–430, doi:10.5194/cp-6-415-2010, 2010. 1306, 1310, 1331

Burrows, C. J. and Russell, J. B.: Aranuian vegetation history of the Arrowsmith Range, Canterbury I. Pollen diagrams plant macrofossils, and buried soils from Prospect Hill, New Zeal. J. Bot., 28, 323–345, 1990. 1318, 1319

Braconnot, P., Otto-Bliesner, B., Harrison, S., Joussaume, S., Peterchmitt, J.-Y., Abe-Ouchi, A., Crucifix, M., Driesschaert, E., Fichefet, Th., Hewitt, C. D., Kageyama, M., Kitoh, A., Laîné, A., Loutre, M.-F., Marti, O., Merkel, U., Ramstein, G., Valdes, P., Weber, S. L., Yu, Y., and Zhao, Y.: Results of PMIP2 coupled simulations of the Mid-Holocene and Last Glacial Maximum – Part 1: experiments and large-scale features, Clim. Past, 3, 261–277, doi:10.5194/cp-3-261-2007, 2007. 1306, 1309, 1318

Gordon, C., Cooper, C., Senior, C. A., Banks, H., Gregory, J. M., Johns, T. C., Mitchell, J. F. B., and Wood, R. A.: The simulation of SST, sea-ice extents and ocean heat transports in a version of the Hadley Centre Model without flux adjustments, Clim. Dyn., 16, 147–168, 2000. 1309

Harris, W. F.: Palaeo-ecological evidence from pollen and spores, Proceedings of the New Zealand Ecological Society, 10, 38–44, 1963. 1319

Horrocks, M. and Ogden, J.: Fine resolution palynology of Gibsons' Swamp, central North Island, New Zealand, since c 13000 B.P. New Zeal J. Bot., 36, 273–283, 1998. 1319

Jane, G. T. and Green, T. G. A.: Episodic forest mortality in the Kaimai Ranges, North Island, New Zealand, New Zeal J. Bot., 21, 21–31, 1983. 1319

Jane, G. T. and Green, T. G. A.: Ecological aspects of climate patterns within the Kaimai Ranges, North Island, New Zealand, New Zeal J. Ecol., 7, 183–197, 1984. 1319

Joussaume, S. and Taylor K. E.: The Paleoclimate Modeling Intercomparison Project: Proceedings of the third PMIP workshop, in: WCRP-111, WMO/TD-1007, edited by: Braconnot, P., Canada, 4–8 October 1999, 25–42, 2000. 1306

K-1 model developers: K1 coupled GCM (MIROC) description, edited by: Hasumi, H. and Emori, S., 34 pp., available at: http://www.ccsr.u-tokyo.ac.jp/kyosei/hasumi/MIROC/tech-repo.pdf, 2004. 1309

Kalnay, E., Kanamitsu, M., Kistler, R., Collins, W., Deaven, D., Gandin, L., Iredell, M., Saha, S.,

CPD
7, 1301–1337, 2011

New Zealand climate in the Mid-Holocene

D. Ackerley et al.

White, G., Woolen, J., Zhu, Y., Chelliah, M., Ebisuzaki, W., Higgins, W., Janowiak, J., Mo, K. C., Ropelewski, C., Wang, J., Leetmaa, A., Reynolds, R., Jenne, R., and Joseph, D.: The NCEP/NCAR 40-year reanalysis project, B. Am. Meteorol. Soc., 77, 437–471, 1996. 1304

Kidson, J. W.: An automated procedure for the identification of synoptic types applied to the New Zealand region, Int. J. Climatol., 14, 711–721, 1994. 1304

Kidson, J. W.: Relationship of New Zealand daily and monthly weather patterns to synoptic weather types, Int. J. Climatol., 14, 723–737, 1994. 1304

Kidson, J. W.: The utility of surface and upper air data in synoptic climatological specification of surface climatic variables, Int. J. Climatol., 17, 399–413, 1997. 1305, 1310

Kidson, J. W.: An analysis of New Zealand synoptic types and their use in defining weather regimes, Int. J. Climatol., 20, 299–316, 2000. 1304, 1305, 1310, 1315, 1316, 1330

Lamy, F., Hebbeln D., Rohl, U., and Wefer, G.: Holocene rainfall variability in southern Chile: a marine record of latitudinal shifts of the Southern Westerlies, Earth Planet. Sci. Lett., 185, 369–382, 2001. 1320

Leathwick, J. R. and Whitehead, D.: Soil and atmospheric water deficits and the distribution of New Zealand's indigenous tree species, Funct. Ecol., 15, 233–242, 2001. 1319

Legutke, S. and Voss, R.: The Hamburg atmosphere-ocean coupled model ECHO-G. Technical Report 18, German Climate Computer Center (DKRZ) (available online at: http://www.mad.zmaw.de/fileadmin/extern/documents/reports/ReportNo.18.pdf), 1999. 1308

Li, X., Rapson, G. L., and Flenley, J. R.: Holocene vegetational and climatic history, Sponge Swamp, Haast, south-western New Zealand, Quatern Int., 184, 129–138, 2008. 1318, 1319

Lorrey, A., Fowler, A. M., and Salinger, J.: Regional climate regime classification as a qualitative tool for interpreting multi-proxy palaeoclimate data spatial patterns: A New Zealand case study, Palaeogeography, Palaeoclimatology, Palaeoecology, 253, 407–433, 2007. 1304, 1305, 1306, 1321, 1322, 1323

Lorrey, A., Williams, P., Salinger, J., Martin, T., Palmer, J., Fowler, A., Zhao, J. X., and Neil, H.: Speleothem stable isotope records interpreted within a multi-proxy framework and implications for New Zealand palaeoclimate reconstruction, Quatern Int., 187, 52–75, 2008. 1304, 1306, 1319, 1321

Manson, B. R.: The life history of silver beech (Nothofagus menziesii), Proceedings of the New Zealand Ecological Society, 21, 27–31, 1974. 1319

Martin, T. J. and Ogden, J.: The seed ecology of Ascarina Lucida: A rare New Zealand tree adapted to disturbance, New Zeal J. Bot., 40, 397–404, 2002. 1318

Martin, T. J. and Ogden, J.: Experimental studies on the drought, waterlogging, and frost tolerance of Ascarina Lucida Hook. f. (Chloranthaceae) seedlings, New Zealand J. Ecol., 29, 1, 53–59, 2005. 1318

McGlone, M. S. and Bathgate, J. L.: Vegetation and climate history of the Longwood Range, South Island, New Zealand, New Zeal J. Bot., 21, 293–315, 1983. 1319

McGlone, M. S., Neall, V. E., and Clarkson, B. D.: The effect of recent volcanic events and climatic changes on the vegetation of Mt Egmont (Mt Taranaki), New Zealand, New Zeal J. Bot., 26, 123–144, 1988. 1318

McGlone, M. S., Salinger, M. J., and Moar, N. T.: Paleovegetation studies of New Zealand's climate since the Last Glacial Maximum, in: Global climates since the Last Glacial Maximum, edited by: Wright, Jr, H. E., Kutzbach, J. E., Webb III, T., Ruddiman, W. F., Street-Perrott, F. A., and Bartlein, P. J., University of Minnesota Press, Minneapolis, 294–317, 1993. 1318, 1319, 1320

Mullan, A. B.: Southern Hemisphere sea-surface temperatures and their contemporary and lag association with New Zealand temperature and precipitation, Int. J. Climatol., 18, 817–840, 1998. 1304

Neuner, G., Bannister, P., and Larcher, W.: Ice formation and foliar frost resistance in attached and excised shoots from seedlings and adult trees of Nothofagus menziesii, New Zeal J. Bot., 35, 221–227, 1997. 1319

Newnham, R. M., Lowe, D. J., and Green, J. D.: Palynology, vegetation, and climate of the Waikato lowlands, North Island, New Zealand, since c. 18,000 years ago, J. Roy. Soc. New Zeal, 19, 2, 127–150, 1989. 1318

Ogden, J., Stewart, G. H., and Allen, R. B.: Ecology of New Zealand Nothofagus forests, in: The ecology and biogeography of Nothofagus forests, edited by: Veblen, T. T., Hill, R. S., and Read, J., Yale University Press, New Haven, Conneticut, 25–82 pp., USA. 1319

Ohgaito, R. and Abe-Ouchi, A.: The role of ocean thermodynamics and dynamics in Asian summer monsoon changes during the mid-Holocene, Clim. Dynam., 29(1), 39–50, 2007. 1309

Phipps, S. J.: Technical Report: The CSIRO Mk3L climate system model v1.2 *for* Antacrtic Climate and Ecosystems Cooperative Research Centre, 2010. 1307

Randall, D. A., Wood, R. A., Bony, S., Colman, R., Fichefet, T., Fyfe, J., Kattsov, V., Pitman, A., Shukla, J., Srinivasan, J., Stouffer, R. J., Sumi, A., and Taylor, K. E.: Climate Models and Their Evaluation, in: Climate Change 2007: The Physical Science Basis. Contribution of

Working Group I to the Fourth Assessment Report of the Intergovernmental Panel on Climate Change, edited by: Solomon, S., Qin, D., Manning, M., Chen, Z., Marquis, M., Averyt, K. B., Tignor, M., and Miller, H. L.: Cambridge University Press, Cambridge, UK and New York, NY, USA, 2007. 1306

Roeckner, E., Arpe, K., Bengtsson, L., Christoph, M., Claussen, M., Dümenil, L., Esch, M., Giorgetta, M., Schlese, U., and Schulzweida, U.: The atmospheric general circulation model ECHO-G4: model description and simulation of present-day climate, Technical Report, 218, Max Planck Institut für Meteorologie, 1996. 1308

Rojas, M., Moreno, P., Kageyama, M., Crucifix, M., Hewitt, C., Abe-Ouchi, A., Ohgaito, R., Brady, E. C., and Hope, P.: The Southern Westerlies during the last glacial maximum in PMIP2 simulations, Clim. Dynam., 32, 525–548, 2009. 1306

Salinger, M. J.: New Zealand climate I: Precipitation patterns, Mon. Weather Rev., 108, 1892–1904, 1980. 1304

Salinger, M. J.: New Zealand climate II: Temperature patterns, Mon. Weather Rev., 108, 1905–1912, 1980. 1304

Salinger, M. J. and Mullan, A. B.: New Zealand climate: Temperature and precipitation variations and their links with atmospheric circulation 1930–1994, Int. J. Climatol., 19, 1049–1071, 1999. 1304

Schaefer, J. M., Denton, G. H., Kaplan, M., Putnam, A., Finkel, R. C., Barrell, D. J. A, Andersen, B. G., Schwartz, R., Mackintosh, A., Chinn, T., and Schulchter, C.: High-frequency Holocne glacier fluctuations in New Zealand differ from the northern signature, Science, 324, 622–625, 2009. 1319

Singarayer, J. S. and Valdes, P. J.: High-latitude climate sensitivity to ice-sheet forcing over the last 120 kyr, Quatern. Sci. Rev., 29(1–2), 43–55, 2010. 1309

Sturman, A. P., Trewinnard, A. C., and Gorman, P. A.: A study of atmospheric circulation over the South Island of New Zealand (1961–1980), Weather and Climate, 4(2), 53–62, 1984. 1304

Sun, O. J. and Sweet, G. B.: Comparison of frost tolerance of Nothofagus solandri var. cliffortioides (Hook.f.) Poole and Nothofagus menziesii (Hook.f.) Oerst, New Zealand J. Botany, 34, 273–278, 1996. 1319

Tait, A., Henderson, R., Turner, R., and Zheng, Z.: Thin plate smoothing spline interpolation of daily rainfall for New Zealand using a climatological rainfall surface, Inter. J. Climatol., 26, 2097–2115, 2006. 1316

Vandergoes, M. J., Fitzsimmons, S. J., and Newnham, R. M.: Late glacial to Holocene vegetation and climate change in the eastern Takitimu Mountains, western Southland, New Zealand, J. Roy Soc. New Zeal, 21(1), 53–66, 1997. 1318, 1319
Wagner, S., Widmann, M., Jones, J. M., Haberzettl, T., Lücke, A., Mayr, C., Ohlendorf, C., Schäbitz, F., and Zolitschka, B.: Transient simulations, empirical reconstructions and forcing mechanisms for the Mid-Holocene hydrological climate in southern Patagonia, Clim. Dynam., 29, 333–355, 2007. 1306, 1308
Wardle, R.: Using anticyclonicity to determine the position of the Southern Hemisphere westerlies, Geophys. Res. Lett., 30, doi:10.1029/2003GL018792, 2003. 1306
Wolff, J., Maier-Reimer, E., and Legutke, S.: The Hamburg Primitive Equation Model HOPE, in: Technical Report 18, German Climate Computer Center (DKRZ), 1997. 1308

CPD
7, 1301–1337, 2011

Table 1. The frequency of occurrence (%) of the Trough (T), Zonal (Z) and Blocking (B) regimes in the pre-industrial control (PI) and Mid-Holocene (MH) runs for each model. The change in the frequency of occurrence (%) of each regime (DT, DB and DZ) for the MH relative to the PI is also included for each model. Statistically significant ($p \leq 0.05$) changes are denoted with a*.

Regime → Model/Season ↓	T PI	T MH	DT MH-PI	Z PI	Z MH	DZ MH-PI	B PI	B MH	DB MH-PI
DJF									
NCEP	37.6			14.4			48.1		
CSIRO Mk3L	44.0	48.0	4.0*	17.8	13.6	−4.2*	38.2	38.4	0.2
ECHO-G	42.4	39.7	−2.7*	20.1	17.3	−2.8*	37.5	43.0	5.5*
HadCM3_UB	43.6	46.0	2.4*	14.5	11.0	−3.5*	41.9	43.1	1.2
MIROC	43.4	45.3	1.9*	16.0	16.2	0.2	40.6	38.4	−2.2*
MAM									
NCEP	29.9			27.5			42.6		
CSIRO Mk3L	29.0	36.2	7.2*	33.0	29.4	−3.6*	37.9	34.5	−3.4*
ECHO-G	29.0	42.3	13.3*	32.9	22.4	−10.5*	38.2	35.4	−2.8*
HadCM3_UB	27.4	37.7	10.3*	29.0	18.2	−10.8*	43.1	44.1	1.0
MIROC	24.6	33.4	8.8*	31.4	26.9	−4.5*	44.0	39.9	−4.1*
JJA									
NCEP	39.3			29.4			31.3		
CSIRO Mk3L	45.3	45.0	−0.3	19.4	22.2	2.8*	35.3	32.8	−2.5*
ECHO-G	44.6	40.9	−3.7*	18.5	22.3	3.8*	36.8	36.9	0.1
HadCM3_UB	37.9	30.5	−7.4*	17.6	24.2	6.6*	44.4	45.3	0.9
MIROC	44.0	40.6	−3.4*	25.0	23.8	−1.2	31.0	35.6	4.6*
SON									
NCEP	43.1			30.0			26.8		
CSIRO Mk3L	34.6	26.5	−8.1*	35.3	41.1	5.8*	30.1	32.3	2.2*
ECHO-G	38.7	29.8	−8.9*	39.2	48.9	9.7*	22.0	21.3	−0.7
HadCM3_UB	42.8	38.1	−4.7*	39.0	47.0	8.0*	18.3	15.0	−3.3*
MIROC	46.8	39.5	−7.3*	29.7	36.0	6.3*	23.7	24.7	1.0

CPD
7, 1301–1337, 2011

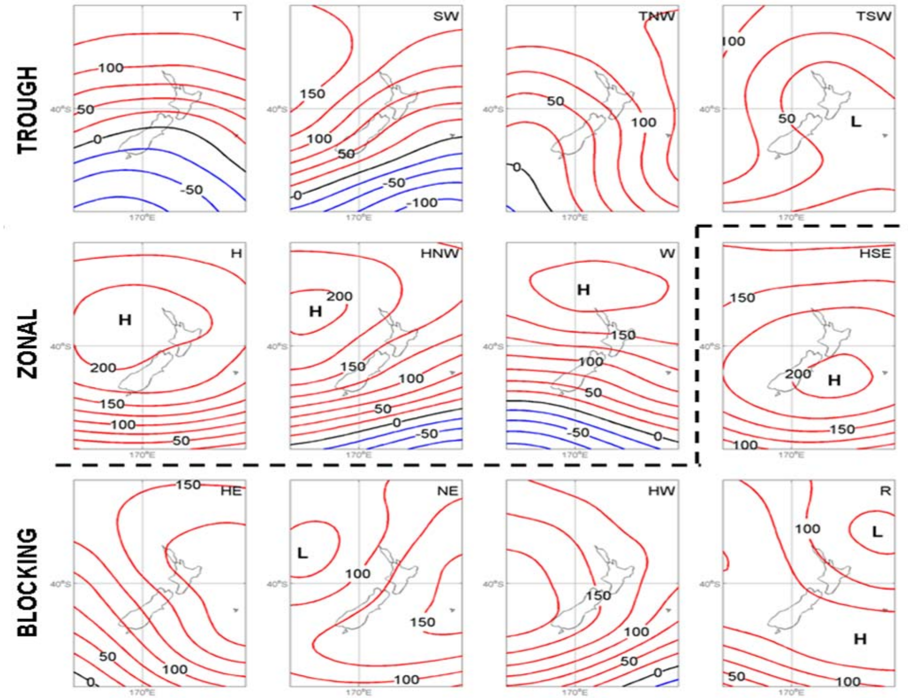

Fig. 1. The twelve Kidson weather types, shown as average patterns of 1000 hPa geopotential height (analogous to mean sea-level pressure). Names for the types are indicated in the top right of each panel (see text for details). The three regimes are indicated at the left: the top row is the trough regime, the first three in the second row are the zonal regime and the rest form the blocking regime. See Kidson (2000) for further details.

CPD
7, 1301–1337, 2011

Title Page
Abstract | Introduction
Conclusions | References
Tables | Figures
◂◂ | ▸▸
◂ | ▸
Back | Close
Full Screen / Esc
Printer-friendly Version
Interactive Discussion

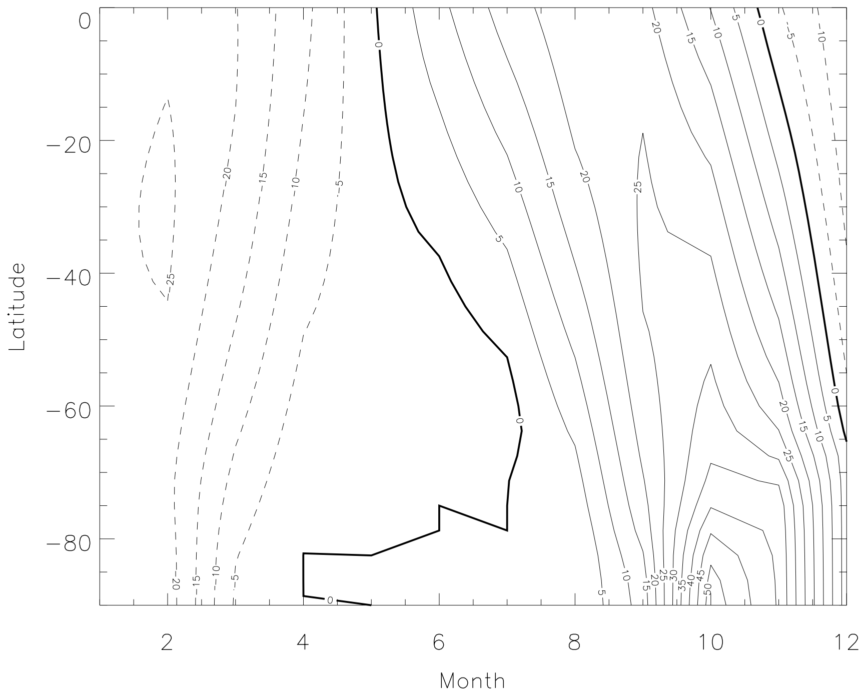

Fig. 2. The calculated difference in zonal, seasonal mean insolation for the Mid-Holocene relative to the pre-industrial control (Wm^{-2}) from Ackerley and Renwick (2010). Positive (negative) values are indicated by the solid (dashed) lines. The zero line is the thick black line.

CPD
7, 1301–1337, 2011

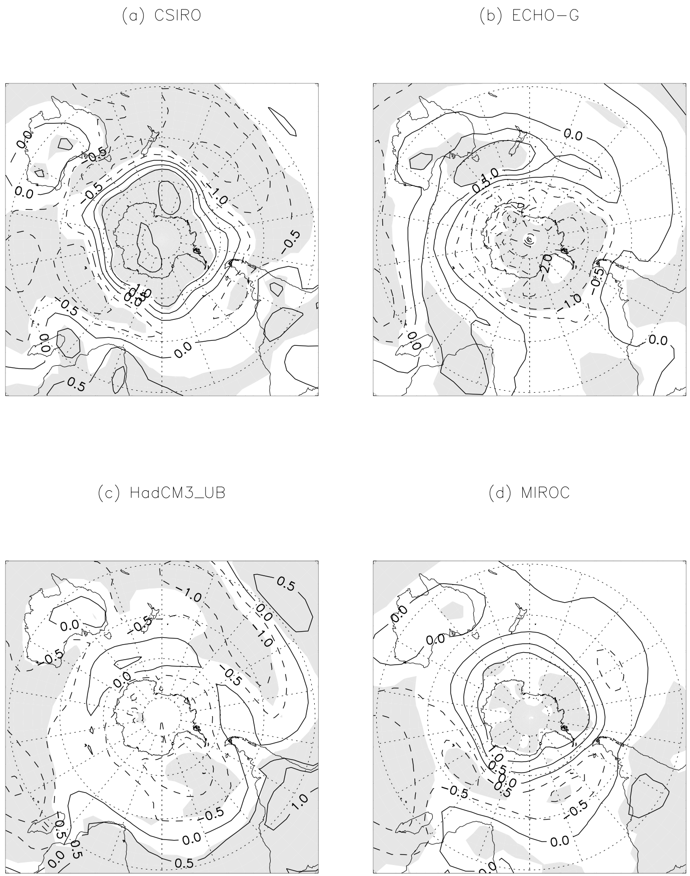

Fig. 3. The difference in DJF mean sea level pressure (hPa) for the Mid-Holocene relative to the pre-industrial control run for **(a)** CSIRO Mk3L, **(b)** ECHO-G, **(c)** HadCM3_UB and **(d)** MIROC. Solid (dashed) contours indicate positive (negative) changes in pressure. Statistically significant changes in SLP ($p \leq 0.05$) are shaded grey.

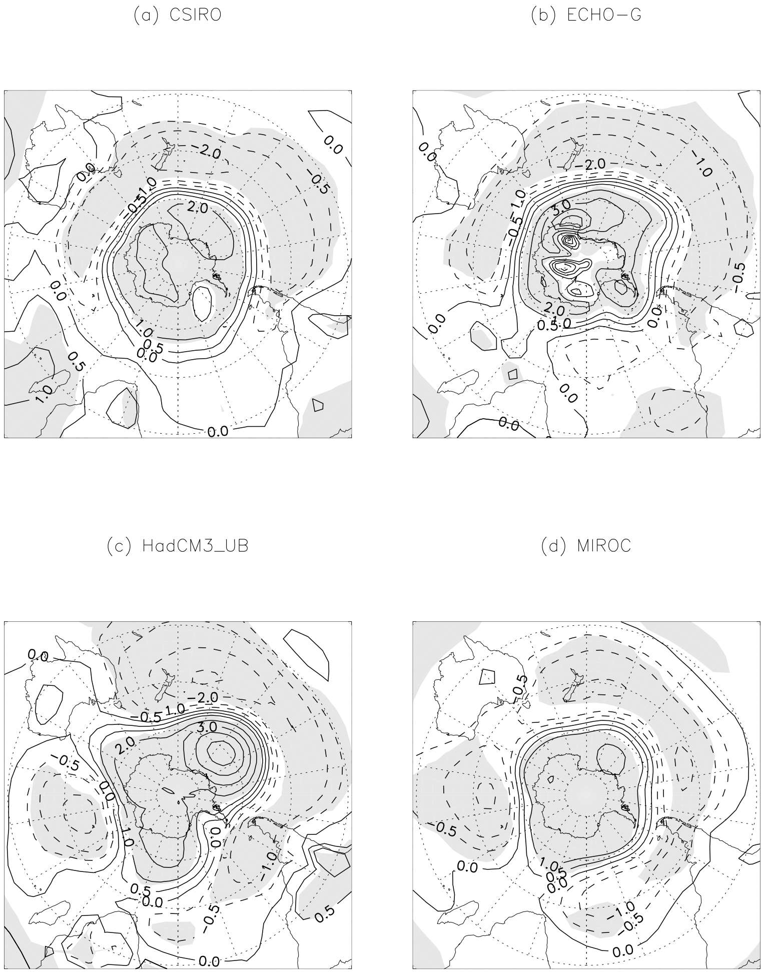

Fig. 4. The same as Fig. 3 except for MAM.

CPD
7, 1301–1337, 2011

New Zealand climate in the Mid-Holocene

D. Ackerley et al.

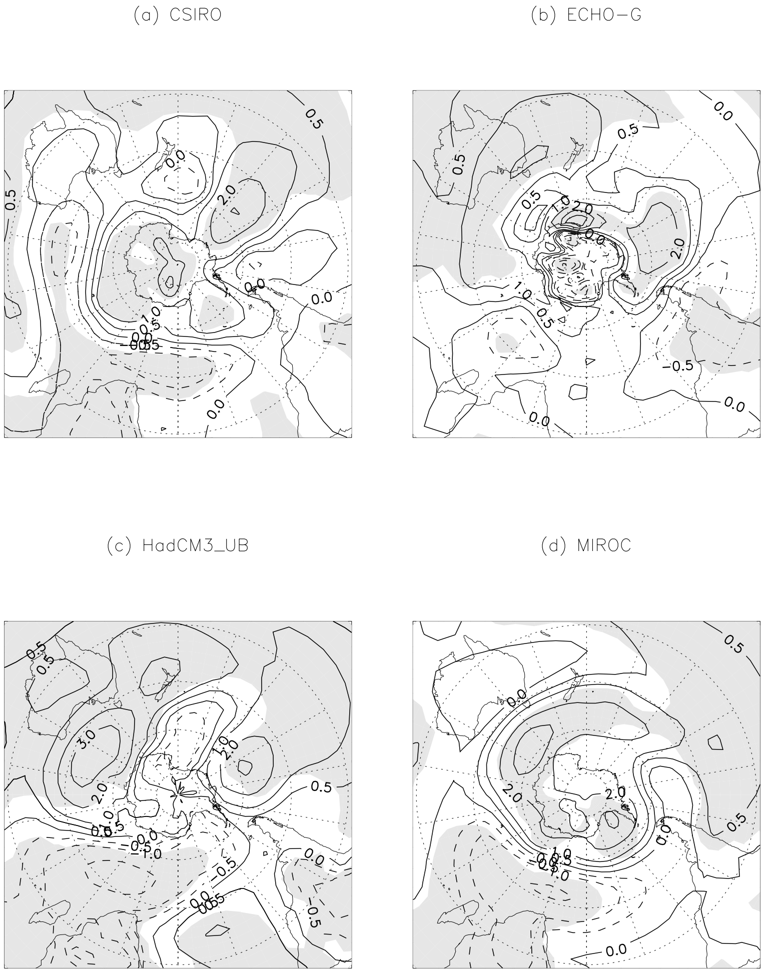

Fig. 5. The same as Fig. 3 except for JJA.

CPD
7, 1301–1337, 2011

New Zealand climate in the Mid-Holocene

D. Ackerley et al.

Title Page
Abstract Introduction
Conclusions References
Tables Figures
◂ ▸
Back Close
Full Screen / Esc
Printer-friendly Version
Interactive Discussion

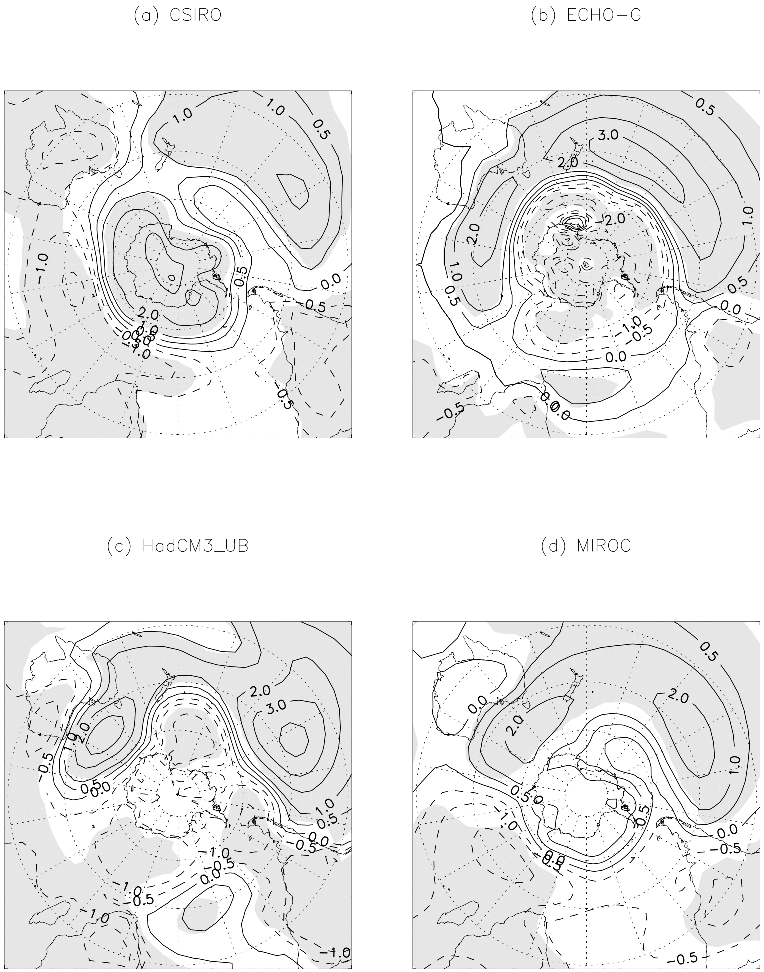

Fig. 6. The same as Fig. 3 except for SON.

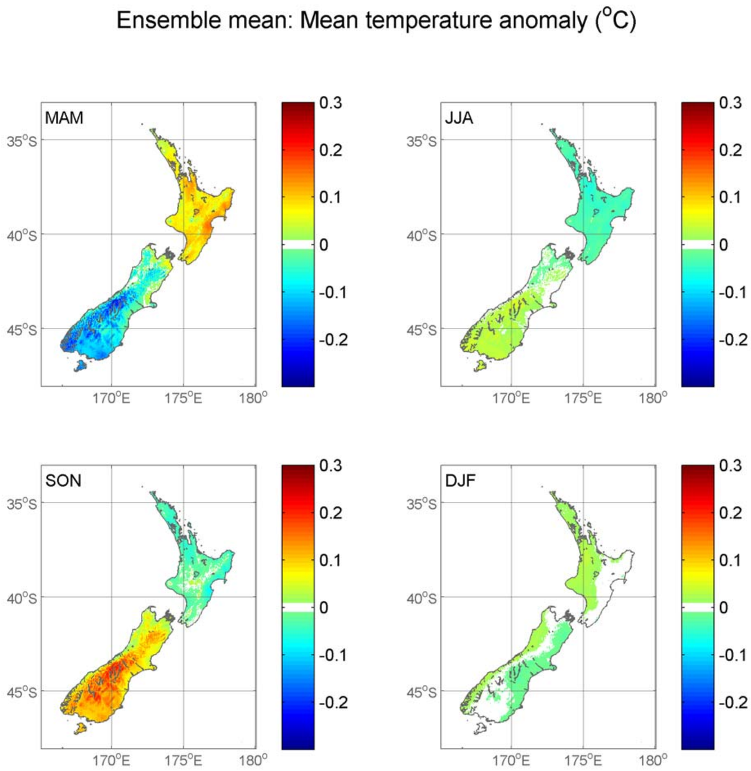

Fig. 7. The ensemble mean change in surface air temperature (°C) associated with the changes in the frequencies of occurrence given in Table 1 for the MH relative to the PI during MAM, JJA, SON and DJF.

CPD
7, 1301–1337, 2011

New Zealand climate in the Mid-Holocene

D. Ackerley et al.

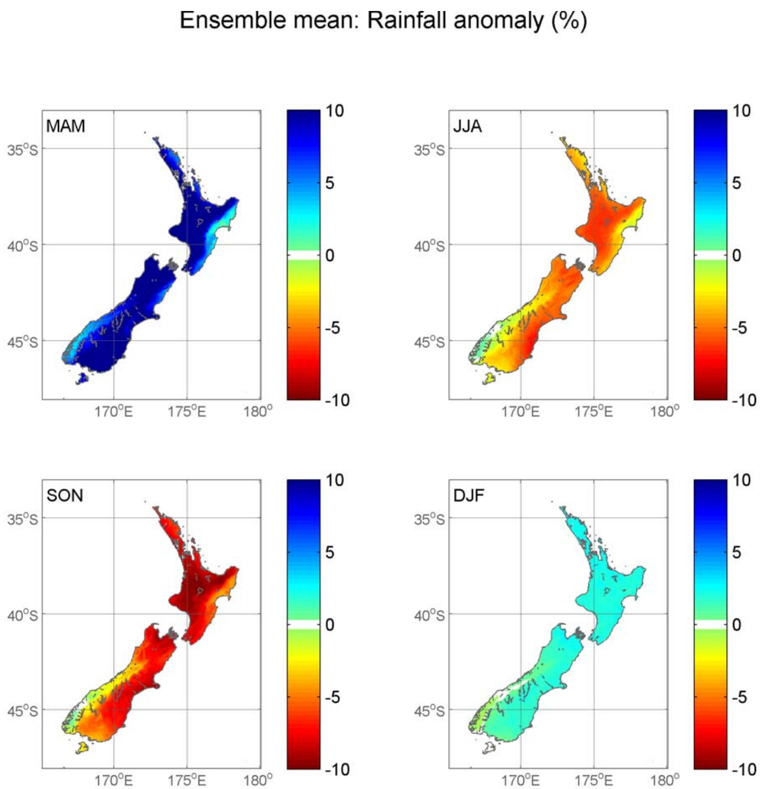

Fig. 8. The same as Fig. 7 except for the precipitation anomaly (%).

CPD
7, 1301–1337, 2011

New Zealand climate in the Mid-Holocene

D. Ackerley et al.

Title Page
Abstract Introduction
Conclusions References
Tables Figures
◀I ▶I
◀ ▶
Back Close
Full Screen / Esc
Printer-friendly Version
Interactive Discussion